Molecular Therapy
Oncolytics
Review

A brief review of reporter gene imaging in oncolytic virotherapy and gene therapy

Susanna C. Concilio,[1] Stephen J. Russell,[1] and Kah-Whye Peng[1]

[1]Department of Molecular Medicine, Mayo Clinic, Rochester, MN 55905, USA

Reporter gene imaging (RGI) can accelerate development timelines for gene and viral therapies by facilitating rapid and noninvasive *in vivo* studies to determine the biodistribution, magnitude, and durability of viral gene expression and/or virus infection. Functional molecular imaging systems used for this purpose can be divided broadly into deep-tissue and optical modalities. Deep-tissue modalities, which can be used in animals of any size as well as in human subjects, encompass single photon emission computed tomography (SPECT), positron emission tomography (PET), and functional/molecular magnetic resonance imaging (f/mMRI). Optical modalities encompass fluorescence, bioluminescence, Cerenkov luminescence, and photoacoustic imaging and are suitable only for small animal imaging. Here we discuss the mechanisms of action and relative merits of currently available reporter gene systems, highlighting the strengths and weaknesses of deep tissue versus optical imaging systems and the hardware/reagents that are used for data capture and processing. In light of recent technological advances, falling costs of imaging instruments, better availability of novel radioactive and optical tracers, and a growing realization that RGI can give invaluable insights across the entire *in vivo* translational spectrum, the approach is becoming increasingly essential to facilitate the competitive development of new virus- and gene-based drugs.

INTRODUCTION

Engineered viruses have emerged as the workhorses of oncolytic virotherapy (OV) and gene therapy.[1–4] To date, one herpes simplex-derived oncolytic virus (Imlygic), three adeno-associated virus (AAV) gene therapies (Glybera, Luxturna, and Zolgensma) and five retro- or lentiviral cellular gene therapies (Strimvelis, Kymriah, Tecartus, Yescarta, and Zynteglo) have gained marketing approval in the United States and/or the European Union. Ongoing clinical development of viral vectors for other disease indications is expected to benefit greatly from incorporating reporter gene imaging (RGI) to shorten development timelines by providing critical information on the biodistribution, magnitude, and duration of viral gene expression. RGI employs a variety of tracers and imaging modalities to detect the expression of reporter-gene-encoded proteins at their site of production in living animals. This review provides a succinct explanation of the following common RGI modalities and transgenes, emphasizing their relative strengths and limitations: three deep-tissue modalities (single photon emission computed tomography [SPECT], positron emission tomography [PET], and functional/molecular magnetic resonance imaging [f/mMRI]) and four optical imaging modalities (fluorescence, bioluminescence, Cerenkov luminescence, and photoacoustic imaging [PAI]).

We have focused exclusively on reporter genes that have been incorporated into oncolytic viruses or viral gene therapy vectors being developed for direct *in vivo* gene transfer (Figure 1). Not covered are the topics of imaging for *ex vivo* cellular therapies or imaging with quantum dots, nanoparticles, fluorescent dyes, contrast agents, or imaging of endogenously expressed proteins such as the dopamine D2 receptor (D2R), somatostatin receptor 2 (SSTR2), prostate-specific membrane antigen (PSMA), or transferrin receptor-1 (Tfr), but resources are provided for the reader's interest.[5–26] Additionally, detailed reviews of imaging for OV and gene therapy are recommended.[27–29]

THE NECESSITY OF *IN VIVO* IMAGING

Oncolytic virotherapy and gene therapy depend on adequate delivery of the viral vector and effective targeting to the tissues of interest. Insufficient transduction of target tissues, leading to insufficient transgene expression, is often the primary limitation affecting the potency of these therapies. RGI can be helpful in identifying these problems in living animals, especially because it can be repeated at multiple time points in a single experimental animal, avoiding the need for euthanasia and analysis of necropsy material at multiple time points. For example, employing an AAV-9 vector encoding the sodium iodide symporter (NIS) reporter gene, Moulay et al.[30] used SPECT/computed tomography (CT) imaging to determine that intracoronary perfusion is a suboptimal method for transduction of heart muscles in research canines but that this can be remedied by using a novel spiral catheter and a new cardiac muscle injection technique. Such an example illustrates that it is essential to monitor and quantify infection and therapeutic gene expression throughout the course of treatment, especially in preclinical studies using large animal models. Most gene products cannot be assessed via blood assays and require other methods, such as invasive biopsies or non-invasive imaging with reporter genes. Besides the obvious drawbacks of

https://doi.org/10.1016/j.omto.2021.03.006.

Correspondence: Kah-Whye Peng, Department of Molecular Medicine, Mayo Clinic, Rochester, MN 55905, USA.
E-mail: peng.kah@mayo.edu

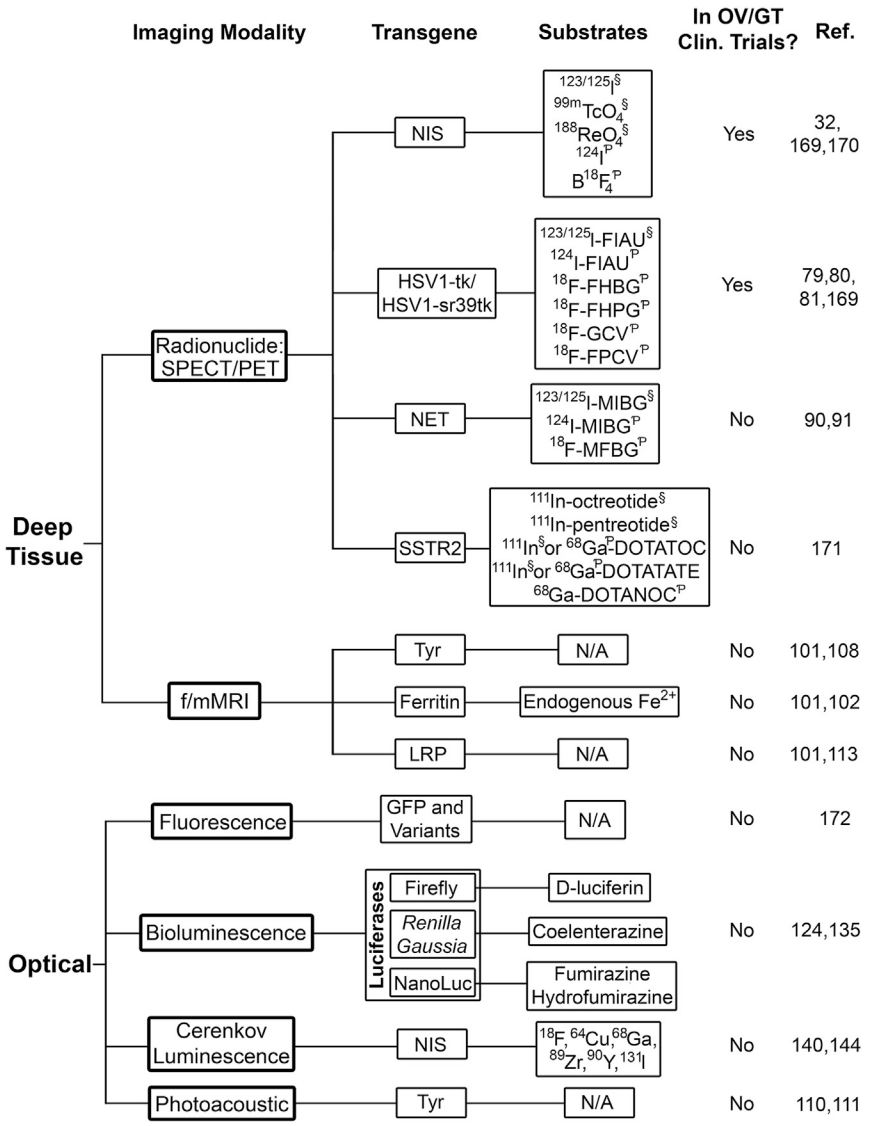

Figure 1. Reporter gene imaging in oncolytic virotherapy and gene therapy

Reporter genes are organized by imaging modality. Commonly used imaging substrates are indicated, as well as the use of reporter genes in human clinical trials of oncolytic virotherapy or gene therapy. §SPECT radiotracer; ᴾPET radiotracer. Abbreviations: SPECT, single photon emission computed tomography; PET, positron emission tomography; NIS, sodium iodide symporter; HSV1-tk1, herpes simplex virus 1 thymidine kinase; FIAU, 1-(2-deoxy-2-fluoro-1-D-arabinofuranosyl)-5-iodouracil; FHBG, 9-(4-fluoro-3-[hydroxymethyl]butyl)guanine; FHPG, 9-[(3-fluoro-1-hydroxy-2-propoxy)methyl]guanine; GCV, ganciclovir; FPCV, 8-fluoropenciclovir; NET, norepinephrine transporter; MIBG, meta-iodobenzylguanidine; MFBG, meta-fluorobenzylguanidine; SSTR2, somatostatin receptor 2; DOTATOC, (DOTA^0-Phe1-Tyr3)octreotide; DOTATATE, DOTA^0-Tyr3-octreotate; DOTANOC, DOTA-1-Nal(3)-octreotide; f/mMRI, functional or molecular magnetic resonance imaging; Tyr, tyrosinase; N/A, not applicable; LRP, lysine-rich protein; GFP, green fluorescent protein.

patient/animal discomfort and surgical risks, biopsies only provide a snapshot at one time point in a single tissue.[31] To truly understand the pharmacokinetics and pharmacodynamics of a viral vector, repeated non-invasive imaging across the entire body is necessary.[32] If only the tissues of interest are sampled, infection of unsampled tissues may be missed, leading to possible side effects that could not be explained or addressed without extensive biopsies. Tracking gene expression over long periods is especially critical for gene therapy, which usually aims for lifelong expression of a therapeutic gene. Longitudinal tracking is imperative to prove the safety and efficacy of such therapies. Early gene therapy studies suffered from a lack of effective tracking mechanisms: did the therapy fail because the vector did not infect the right tissue or the transgene did not express? Or, what caused toxicity: the vector, too much transgene expression, or infection of off-target tissues?[33–35] The use of reporter genes in these systems would answer these key questions.

Challenges to widespread use of reporter genes lie mainly in the technology required to image them: imaging agents and machines can be costly, and specialized training may be needed to handle these agents. However, facilities capable of producing short half-life radiotracers in-house are proliferating, and imaging instruments are becoming cheaper and more widespread, expanding access for both preclinical and clinical applications. Many manufacturers have also designed the imaging machines to be capable of multi-modality imaging, incorporating highly sensitive CT imaging for anatomical location of tissues to complement SPECT or PET modalities. With more centers adopting noninvasive imaging technologies, and increasing attention being given to the "three Rs" in animal research (replace, reduce, refine), RGI must become a fundamental step in virus drug development, as it is an invaluable tool to assess virus spread, infection, persistence, and efficacy.

DEEP-TISSUE IMAGING

Several deep-tissue molecular imaging modalities exist, though the most commonly used are CT, SPECT, PET, MRI, and f/mMRI. CT uses a series of X-rays to generate high-resolution 3D images.[36] SPECT is a type of gamma scintigraphy where individual planar images generated by gamma photons emitted from radiotracers are compiled into a 3D volumetric image via CT.[37] Upon radioactive decay, SPECT radiotracers emit a single photon, with emission in any direction occurring with equal probability.[38] This characteristic necessitates strict collimation to ensure captured photons are directly from the decay event to maintain resolution, which increases the dose

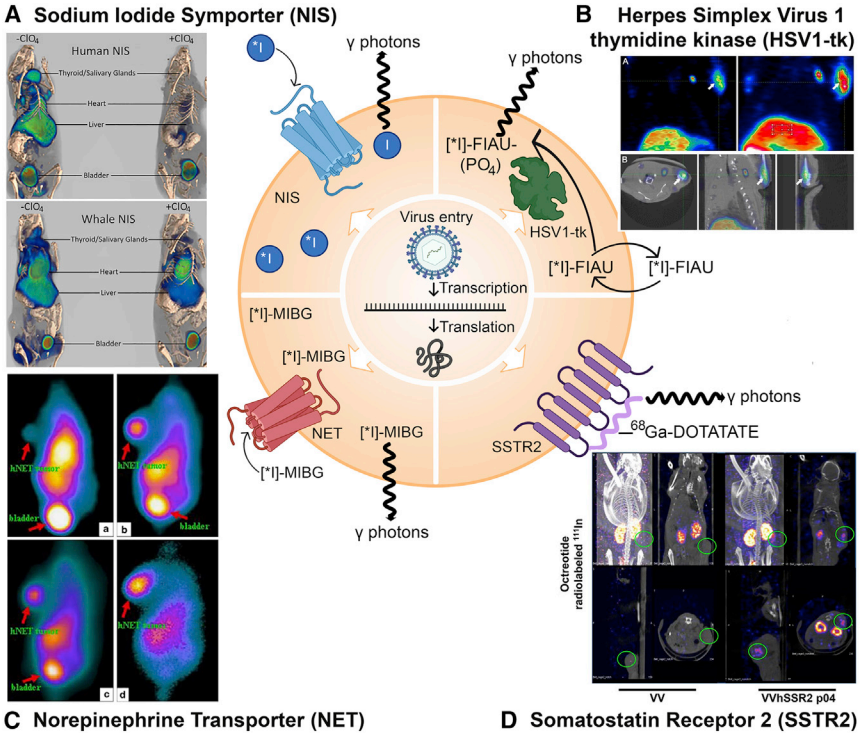

Figure 2. Mechanisms of radionuclide imaging (SPECT/PET) reporter genes and examples from oncolytic virotherapy and gene therapy studies

(A) NIS expressed on the cell surface concentrates *I (*I indicates it can be ^{123}I, ^{124}I, ^{125}I, or ^{131}I) radiotracer into the cell. Decay of *I radiotracers directly releases (^{123}I/^{125}I/^{131}I) or leads to the release (^{124}I) of gamma (γ) photons for SPECT or PET imaging. Imaging panel: 3D reconstruction of PET/CT imaging of mice infected with AAV-9-CAG-human NIS or minke whale NIS in the absence or presence of the NIS inhibitor perchlorate (ClO_4). (B) HSV1-tk: Radiolabeled substrates like [*I]-FIAU can pass in and out of the cell until they are phosphorylated by HSV1-tk to yield [*I]-FIAU-PO_4, which becomes trapped intracellularly. Upon radioactive decay, *I releases γ photons for capture via SPECT/PET. Imaging panel: 9-[4-[^{18F}] fluoro-3-(hydroxymethyl) butyl] guanine (^{18}F-FHBG) uptake in the liver and injection site (arrow) of a self-complementary recombinant AAV-3 vector expressing HSV1-tk and kallistatin. (A) depicts coronal slices of an animal's PET imaging (left) and image of maximum intensity projection (right). (B) depicts transverse, coronal, and sagittal images of the PET/CT. (C) NET: NET transports radiolabeled norepinephrine analogs like [*I]-meta-iodobenzylguanidine (*I-MIBG) into the cell, where γ photons are released upon radioactive decay. Imaging panel: HepG2 tumors in mice infected with an adenovirus expressing NET. ^{131}I γ-camera images 30 min (a), 1 h (b), 4 h (c), and 24 h (d) after radiotracer administration. Radiotracer collects in the bladder non-specifically for excretion. (D) SSTR2: Radiolabeled peptides (such as ^{68}Ga-DOTATE) bind to the SSTR2 receptor and γ photons are released upon radioactive decay. SSTR2 is the only nuclear transgene depicted which cannot amplify its signal due to the 1:1 receptor:peptide binding stoichiometry. Imaging panel: Infection of HT29 tumors with oncolytic vaccinia virus expressing SSTR2 (VV-SSR2) and SPECT imaging with ^{111}In-octreotide 4 days after virus treatment. Figure made with BioRender (https://biorender.com/) and Photoshop CC 2019. Protein shapes are artistic interpretations. Permissions for imaging panels: (A) From Concilio et al.[42] and reproduced under CC Attribution-NonCommercial-NoDerivs License (https://creativecommons.org/licenses/by-nc-nd/4.0/). (B) From Liu et al.[43] and reproduced under CC Attribution License (https://creativecommons.org/licenses/by/4.0/). (C) From Jia et al.[44] and reproduced with licensed permission. (D) From Wang et al.[45] and reproduced with permission from the journal; this research was originally published in *JNM*.

of radioisotope given to achieve sufficiently high signals and imaging.[38] PET imaging is more sensitive and has higher resolution than SPECT due to the unique physics of positron decay and subsequent signal analysis by the detector. Positrons emitted from the nucleus of a radionuclide such as ^{18}F travel a short distance and combine with an electron, resulting in an annihilation reaction. Two 511-keV photons are emitted roughly 180° apart and are detected as a coincident event when they strike opposing detectors simultaneously.[39] It is the requisite simultaneous detection of both photons that provides PET with superior signal-to-background resolution over SPECT.[40] SPECT and PET are often combined with CT for co-registered anatomical and functional imaging.[36] MRI uses strong magnetic fields and radio waves to excite the nuclear spin energy transition of targeted molecules, most frequently hydrogen.[41] The rate of relaxation from the excited state varies per tissue density, and this difference allows for high-resolution imaging.[41] f/mMRI is used to enhance the anatomical data obtained via MRI with physiological data relating to a biological process. However, the sensitivity of f/mMRI for available imaging agents is poor compared to optical imaging and radionuclide imaging (RI).[28] Other drawbacks to MRI are cost of the machines and the time required for imaging (15–90 min).

The following sections are arranged by reporter gene instead of imaging modality, since most deep-tissue imaging transgenes can be used for several modalities depending on the substrate.

RI

NIS

NIS imaging is the most mature RGI method for monitoring gene and viral therapies in human clinical trials. NIS mediates the concentration of iodide into the thyroid gland for thyroid hormonogenesis. NIS can transport several other monovalent anions that can be used for both SPECT and PET (Figure 2A).[46,47] NIS is the most common human reporter gene used, and a plethora of viruses have been engineered to express NIS.[48–54] Many pre-clinical and clinical trials have shown that virally delivered NIS can be used to accurately track viral infection and spread in the tumor, as well as track tumor response to treatment.[55] Several gene therapy studies have displayed the utility of NIS for longitudinal *in vivo* imaging of adenovirus and AAV gene therapies to identify biodistribution and durability of gene expression.[30,56–62] NIS imaging was also shown to be more sensitive and longer lasting than imaging with herpes simplex virus 1 thymidine kinase (HSV1-tk) (discussed below).[60] Development of novel NIS-compatible PET

radiotracers, like ^{18}F-tetrafluoroborate, is likely to replace ^{123}I or $^{99\,m}TcO_4$ SPECT imaging with NIS in the near future due to the superior resolution and sensitivity of PET imaging.[63–65] The half-life of ^{18}F is extremely short (109.7 min), greatly reducing long post-procedure quarantines while the radiotracer is excreted. Studies of ^{18}F-tetrafluoroborate in healthy volunteers show safety, feasibility, and high sensitivity, significantly improving resolution of NIS RGI.[66]

NIS is also unique in the RGI field, as many species of the NIS gene have been sequenced or cloned, enabling RGI in many animal models with the native NIS protein.[67,68] NIS is present in all vertebrates, enabling species-specific NIS vector development for the vast majority of model systems.[69] This has allowed longitudinal imaging in immune-competent small and large animal models due to the lack of immune response against a self-protein reporter gene. Of particular interest, NIS has enabled tracking of OV, cell, and gene therapies in large animal models, the importance of which is discussed later.[30,61,70–76] The moderate sensitivity and excellent specificity of NIS *in vivo* imaging requires fewer animals for small and large animal studies, reducing animal use and costs and expediting pre-clinical and translational research.

Several challenges to NIS imaging include endogenous NIS expression, efflux of radiotracer from NIS-expressing cells, and low transduction/expression of the NIS transgene in transduced target tissues. The concentration of radioisotopes in non-target tissues that naturally express NIS, such as the thyroid, salivary glands, and stomach, makes interpretation and quantitation of NIS signals technically difficult if the transduced tissue is in the vicinity of endogenous NIS-expressing tissues. Several studies have explored ways to improve NIS expression or block endogenous NIS expression to address the above concerns.[77–80] For example, to facilitate imaging of transduced hepatocytes, animals are fed barium sulfate to delineate the stomach/gastrointestinal tract and mask some of the endogenous NIS signal in the gastric mucosa in mice and pig models after AAV gene transfer.[79] A recent study by our group investigated the feasibility of reducing uptake by endogenous NIS via use of the NIS inhibitor perchlorate and a perchlorate-resistant NIS variant from minke whale (*B. acutorostrata scammoni*).[42] Combination of minke whale NIS and perchlorate pretreatment resulted in superior imaging using low levels of AAV-9 transduction in mice with SPECT/CT and PET/CT while significantly reducing uptake in endogenous NIS-expressing tissues.[42] NIS continues to grow in popularity in both preclinical and clinical settings due to its human origin, sensitivity, SPECT and PET utility, label-free radiotracers, and persistence of expression.

HSV1-tk

The next most advanced RGI method for OV and gene therapy in human clinical trials utilizes HSV1-tk. HSV1-tk can phosphorylate non-toxic prodrugs like purine nucleotide derivatives and acyclovir derivatives to trap them in cells, where the toxic forms can be used for radioisotope imaging or radiotherapy (Figure 2B).[27] Since HSV1-tk was one of the first reporter genes investigated, it enjoys a wide breadth of PET and SPECT tracers, as well as mutant forms, such as HSV1-sr39tk, which has enhanced *in vivo* activity.[27,29,81,82] Though HSV1-tk imaging is successful in most small animal models, the results in clinical trials have been mixed.[29,83–86] Investigations into the use of HSV1-tk for human imaging are meager: out of the ten active or recruiting clinical trials currently registered with ClinicalTrials.gov using a virus expressing HSV1-tk, only one plans to perform HSV1-tk imaging (ClinicalTrials.gov: NCT04313868). The paucity of translational application of HSV1-tk for imaging hinders accurate assessment of its potential use in humans. Clinical trials should make every effort to include at least one round of imaging to assess virus spread and infection. Longitudinal imaging would reveal the optimal windows for suicide gene therapy and improve the efficacy of HSV1-tk cancer gene therapy. AAV gene therapy has been quantified in rodents and non-human primates using HSV1-tk PET imaging.[43,87] As a non-human protein, HSV1-tk could provoke an immune response, making it an unlikely candidate for long-term imaging, as would be needed for gene therapy.[88]

Norepinephrine transporter (NET)

NET is a Na^+/Cl^--dependent membrane protein that transports norepinephrine, epinephrine, and dopamine into the cell. The human protein (hNET) has been used as a reporter gene for SPECT and PET with several radiotracers, primarily meta-iodobenzylguanidine (MIBG), which is already approved by the US Food and Drug Administration (FDA) (Figure 2C).[89] NET has been used for nuclear imaging or radiotherapy with vaccinia virus, adenovirus, and herpes virus.[44,90,91] Use of endogenous NET for tumor imaging is still under clinical development and use, but further use of NET for imaging of OV has not been reported beyond the above-mentioned studies, likely due to the existence of other reporter genes with better expression profiles and radiotracer availability.[92,93]

SSTR2

SSTR2 is one of the receptors for the peptide hormone somatostatin and is highly expressed on neuroendocrine cells and others, where it is involved in neurotransmission, hormone secretion, and cell proliferation.[27,94] The human protein (hSSTR2) has been used for SPECT imaging with indium-111-labeled synthetic peptide substrates such as octreotide, pentetreotide, and lanreotide, or PET imaging with gallium-68-labeled peptides (Figure 2D).[95] SSTR2 has been inserted into adenovirus and oncolytic vaccinia, where long-term tracking of viral infection and persistence was shown to be feasible in several tumor types.[32,45,96–99] SSTR2 has also been used to track AAV gene therapy, where it permitted PET imaging 6 months post-treatment.[100] The major drawbacks of SSTR2 are endogenous expression, which can reduce diagnostic efficacy, and that each receptor can only bind one radiolabeled ligand, preventing signal amplification and thus limiting imaging sensitivity.[45,101]

MRI

Ferritin

Ferritin is an endogenous intracellular protein that binds and coverts labile Fe^{2+} iron to the stable and non-toxic Fe^{3+} form for storage (Figure 3A).[105] Iron is an ideal MRI contrast agent, so ferritin

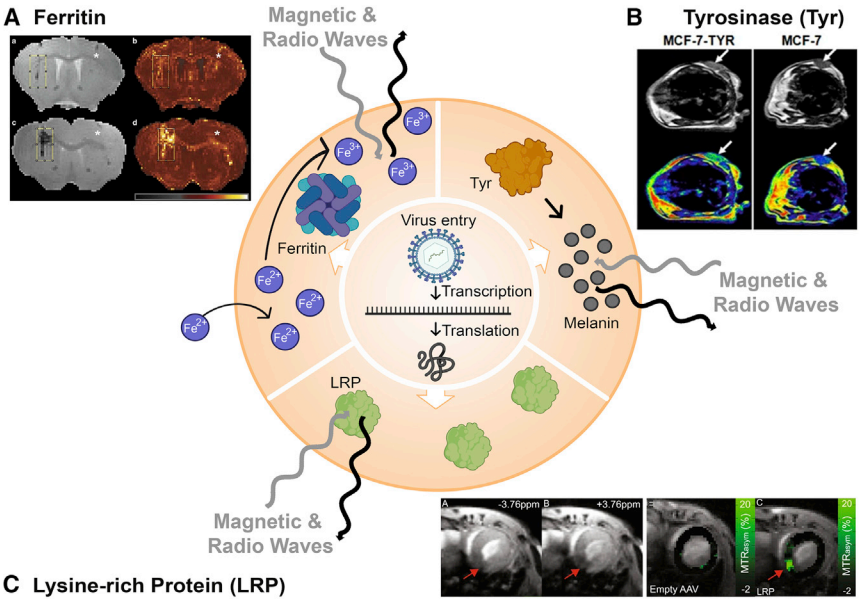

Figure 3. Mechanisms of functional/molecular magnetic resonance imaging (f/mMRI) reporter genes and examples from oncolytic virotherapy and gene therapy studies

(A) Ferritin: Iron cations captured by ferritin induce differences in weighted MRI images. Imaging panel: MRI imaging of (a and b) 25 million particles or (c and d) 100 million particles of HSV-1 expressing ferritin in mouse brain. (B) Tyrosinase: Production of melanin induces differences in weighted MRI images. Imaging panel: MRI imaging of MCF-7 tumors with or without Tyr expression in mice. (C) Lysine-rich protein (LRP): LRP induces differences in weighted MRI images. Imaging panel: MRI chemical exchange saturation transfer (CEST) imaging of murine heart transduced with AAV-9 encoding LRP. Figure made with BioRender (https://biorender.com/) and Photoshop CC 2019. With the exception of ferritin, protein shapes are artistic interpretations. Permissions for imaging panels: (A) From Iordanova et al.[102] and reproduced with licensed permission. (B) From Qin et al.[103] and reproduced under CC Attribution 3.0 Unported License (https://creativecommons.org/licenses/by/3.0/). (C) From Meier et al.[104] and reproduced under CC Attribution 4.0 International License (https://creativecommons.org/licenses/by/4.0/).

overexpression in target cells permits RGI with MRI.[106,107] Ferritin RGI has been tested in lentiviral and AAV gene therapy in rodent brain.[108] HSV1-mediated ferritin expression in mouse brain was sufficient for imaging and permitted quantitative assessment of infectious particles.[102] Ferritin and enhanced green fluorescent protein (GFP) were recently co-expressed in vesicular stomatitis virus (VSV) to assess neural connectivity with MRI.[109] Ferritin is attractive because it does not require any exogenous probes, since it binds to naturally bioavailable iron. However, this approach leads to negative contrast in the MR image, which exhibits low sensitivity (in the mM range) compared to positive contrast approaches like PET (low nM range).[29,110] Further methodologies are required to increase the sensitivity of ferritin RGI.

Tyrosinase (Tyr)

Tyr can be used for fMRI in addition to PET and PAI.[103] Melanin production induced by Tyr expression also increases metal ion chelation, which causes substantial improvement in MRI contrast (Figure 3B).[111] To date, the only studies with Tyr in OV or gene therapy use the vaccinia virus strain GLV-1h68 expressing Tyr and tyrosinase-related protein 1 (Tyrp1), which further enhances melanin production.[112,113] The main problems with Tyr arise from low transgene expression and off-target effects of excess melanin production, such as production of reactive oxygen species and inhibition of virus replication.[105,112–114] Issues arising from excess melanin production can be overcome by using drug-inducible Tyr expression systems, but this adds another layer of genetic and clinical regulatory complication.[113]

Lysine-rich protein (LRP)

LRP is an artificial reporter gene that was generated for use with chemical exchange saturation transfer (CEST) MRI (Figure 3C).[115] CEST MRI relies on radio-frequency-irradiated protons from a source agent (i.e., LRP), which become saturated, exchanging with protons from water in the tissue to decrease bulk water signal on the MRI.[105] CEST imaging has made it to the clinic in the past decade and offers unique windows into physiological changes, such as intracellular and extracellular pH, glucose uptake, and lactate production.[116] LRP was inserted into oncolytic HSV-1 G47Δ and successfully used for CEST MRI without impacting viral replication or oncolytic efficacy.[117] Another study generated an AAV-9 vector encoding LRP to longitudinally track cardiac transduction in mice, with robust imaging achieved 90 days post infection.[104] The sustained expression and lack of observed toxicity bode well for LRP CEST MRI. However, LRP imaging and CEST MRI suffer from low sensitivity and high specific absorption rate (SAR), limiting its clinical use.[105] Novel reporter genes for CEST MRI are needed to spur more widespread use of this interesting imaging technology.

OPTICAL IMAGING

Optical imaging (OI) relies on light in the infrared, visible, or ultraviolet spectrum and thus is best suited for surface imaging and not deep-tissue imaging. OI modalities include fluorescence, bioluminescence, Cerenkov luminescence, and PAI. OI modalities are attractive due their short acquisition times, lower cost, high-throughput abilities, multispectral imaging capabilities, and convenience of use as compared to radioisotopes.[28,89,118] These attributes make OI extremely popular for *in vitro* studies or preclinical studies in small animals. However, light intensity and spatial resolution remain challenges for OI, as emitted photons can be absorbed or scattered by tissue.[28,119] These problems, as well as the potential for immune responses against these non-human proteins, have limited the use of OI reporter genes in the clinic.[28] A thorough review of OI modalities was recently published.[120]

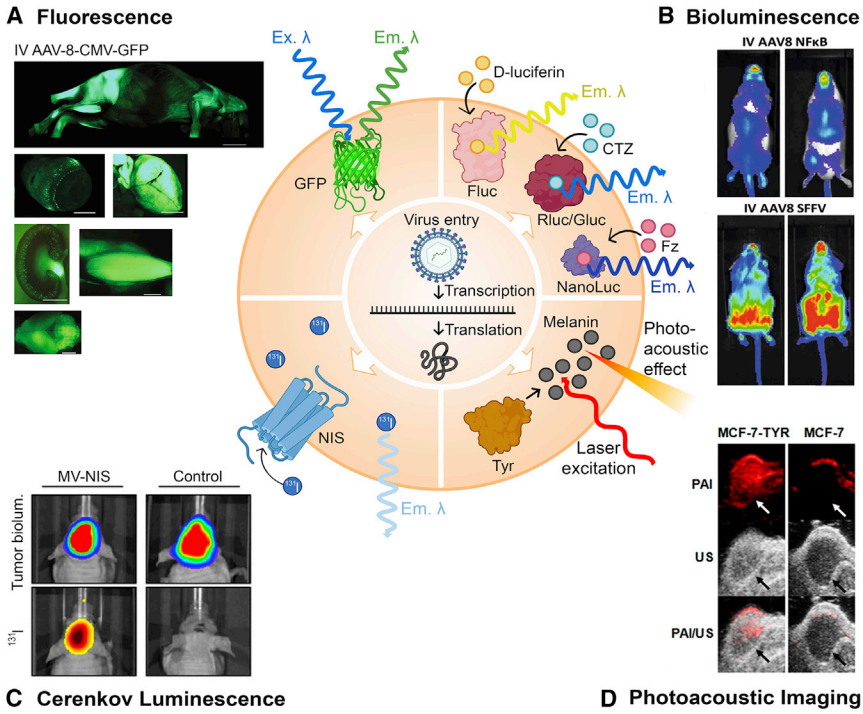

Figure 4. Mechanisms of optical imaging modalities and examples from oncolytic virotherapy and gene therapy studies

(A) Fluorescence: Incident excitation wavelength (Ex. λ) excites the fluorophore within the intracellular GFP and causes an emission wavelength (Em. λ) to be released for detection. Imaging panel: GFP distribution in neonatal mice after intravenous (i.v.) administration of AAV-8-CMV-GFP. Left to right: whole body, eyeball, liver, kidney, muscle, and brain. (B) Bioluminescence: Intracellularly expressed firefly luciferase (Fluc), *Renilla* or *Gaussia* luciferase (Rluc/Gluc), or NanoLuc bind with substrates D-luciferin, coelenterazine (CTZ), or furimazine, respectively, which enters the cell from exogenous sources. Emission wavelengths (Em. λ) are released upon processing of the substrate by luciferase. Imaging panel: Firefly luciferase imaging in mice after i.v. administration of an AAV-8-NFκB-Luc-2A-GFP biosensor or the constitutively expressed control AAV-8-SFFV-Luc-2A-GFP. (C) Cerenkov luminescence: NIS expressed on the cell surface concentrates ^{131}I radiotracer and concentrates it into the cell. Upon radioactive decay, ^{131}I releases light (Em. λ), which can be captured by a charge-coupled camera device. Imaging panel: Medulloblastoma xenografts in mice infected with measles virus expressing NIS (MV-NIS). Top panels are tumor bioluminescence and lower panels are ^{131}I imaging from radiotracer concentrated into the tumor by NIS. (D) Photoacoustic imaging (PAI): Laser light absorbed by tissue is translated to heat and converted into ultrasound waves (photoacoustic effect), which are used for imaging. Tyr produces melanin, which readily absorbs the laser. Imaging panel: PAI and ultrasound imaging (US) of MCF-7 tumors with or without Tyr expression in mice. Figure made with BioRender (https://biorender.com/) and Photoshop CC 2019. With the exception of GFP, protein shapes are artistic interpretations. Permissions for imaging panels: (A and B) From Karda et al.,[121] modified via cropping of the original figure and reproduced under CCA 4.0 International License (https://creativecommons.org/licenses/by/4.0/). (C) From Hutzen et al.[122] and reproduced under CC Attribution License (https://creativecommons.org/licenses/by/2.0). (D) From Qin et al.[103] and reproduced under CC Attribution 3.0 Unported License (https://creativecommons.org/licenses/by/3.0/).

Fluorescence imaging (FI)

FI with reporter genes primarily uses the GFP from the jellyfish *Aequorea victoria* and its variants, such as yellow fluorescent protein (YFP), mCherry, and many others. FI requires incident light at the correct excitation wavelength to reach the fluorophore, which will then release a photon at a distinct emission wavelength to be captured by a specialized charge-coupled device camera (Figure 4A). This negates the need for exogenously applied substrates or imaging agents but is limited by light penetrance into the tissue of interest.[29] Autofluorescence and immunogenicity also limit the sensitivity and persistence of FI. FI can be used to image oncolytic virus infection and spread in murine tumor models and is especially useful for visualizing tumors in explanted orthotopic or subcutaneous models after necropsy. Many oncolytic viruses have been engineered to express GFP or other fluorescent proteins to track viral infection and spread, but IF is best for *in vitro* analysis or requires necropsy of the animal and explanting tissues for analysis under a dissecting microscope.[27] Novel OI genes are constantly being developed, such as infrared fluorescence proteins or the very small endogenously fluorescent protein UnaG, which can be used to monitor gene transfer in AAV vectors, which have limited genetic capacity.[123–125]

Bioluminescence imaging (BLI)

BLI utilizes charge-coupled device cameras to capture light produced by the oxidation of substrates by luciferase enzymes. The most commonly used luciferase enzymes are those from the North American firefly (*P. pyralis*) (Fluc), the sea pansy (*Renilla reniformis*) (Rluc), and the marine copepod (*Gaussia princeps*) (Gluc). Fluc uses D-luciferin as its substrate, along with the cofactors ATP, Mg^{2+}, and O_2, and releases yellow-green light. Both Rluc and Gluc use coelenterazine (CTZ) and release primarily blue light, which is less tissue penetrant than yellow-green light (Figure 4B).[126] Newly developed enzyme variants, such as NanoLuc, and novel substrates continue to improve BLI.[127] Further modifications to NanoLuc or the substrate have expanded imaging options, such as Nano-lanterns, Antares, Antares2, and NanoBiT.[126,128–136] BLI offers an improvement over FI due to a lack of background signal, as only the delivered transgene can catalyze the light-producing reaction with the exogenously supplied substrate. Similar to FI, BLI suffers from poor spatial resolution and depth-dependent signal attenuation, which prevents translation into large animal models and humans.[137]

Though BLI is not used clinically, it is an invaluable tool for preclinical studies. Its ease of use, sensitivity, relative low cost, and relative

lack of toxicity in animal models permits widespread utility in many oncolytic virotherapy and gene therapy platforms.[27,28] BLI can also be quantitative, with studies indicating that viral titers can be correlated with luminosity.[138,139] BLI provides an easy-to-use high-throughput method for estimating viral infection, replication, and persistence in mice, which are fundamental factors to monitor for accurate assessment of any given viral therapy. The limitation is lack of resolution and 3D tomography, making it difficult to discriminate between transduced tissues.

Cerenkov luminescence imaging (CLI)

Cerenkov luminescence is a unique optical phenomenon whereby light is emitted when charged particles, such as positrons (β^+) or electrons (β^-) travel through a dielectric medium faster than the speed of light through that particular medium.[140] The released light is in the ultraviolet-to-visible spectrum and can be captured with sensitive charge-coupled device cameras.[141,142] CLI is attractive due to its optical nature, the detection instrumentation for which is much cheaper than RI modalities, and many of the most suitable radioisotopes are already clinically approved.[120,140,143] Several isotopes permit simultaneous radiotherapy, RI, and CLI.[144] The primary limitations of CLI are low light yield and the high absorption rate of ultraviolet-to-blue light in tissue.[145] These issues hinder the applicability of CLI in clinical settings, but CLI RGI in animals has been reported.[140,146] CLI has been used successfully to image ^{131}I concentration into medulloblastoma xenografts infected with an oncolytic measles virus expressing the NIS in mice (Figure 4C).[122] CLI can allow for imaging of β^- radiotracers, which cannot be detected via other imaging technologies, expanding the repertoire of useful radiotracers.[140]

PAI

Also known as optoacoustic imaging, PAI is a recently developed imaging modality. PAI makes use of the photoacoustic effect by using a short-pulse laser to irradiate the target tissue. Depending on the physical attributes of the tissue, varying amounts of light are absorbed, which causes molecular vibration and the generation of thermoelastic expansion.[120,147] The acoustic waves produced by this process are subjected to less scattering than photons as they travel though tissue, increasing the imaging depth significantly.[120] Contrast agents are sometimes used to enhance molecular specificity.[148,149] To date, only one oncolytic virus has been used for PAI, the previously described vaccinia virus expressing Tyr and Tyrp1, which facilitates melanin production (Figure 4D).[112,113] Melanin is an ideal contrast agent for PAI, as well as MRI, and overexpression in tumors permitted PAI in an animal model.[112] Recently, a calcium and manganese carbonate-coated oncolytic adenovirus was successfully imaged with PAI and MRI in tumor-bearing mice using the bound manganese as the PAI agent.[150] PAI remains underutilized in the OV and gene therapy field but will hopefully expand as more relevant PAI imaging genes are developed.

LARGE ANIMAL IMAGING

The transition from *in vitro* and preclinical *in vivo* studies to clinical trials requires the use of relevant animal models. Particularly for oncolytic virotherapy and gene therapy, adequate assessment of safety and efficacy are essential to the translational process. RGI can play a crucial role in this process, giving insight into otherwise difficult-to-assess parameters like viral spread, replication, and persistence. RGI is already commonly used in small animal models like mice and rats, but it also simplifies the use of large animal models like dogs, pigs, and non-human primates by limiting the need for extensive biopsies and tissue staining of multiple slices. Studies using larger animals with physiologies closer to that of humans are sometimes unavoidable, as they are often better predictors of toxicity or clinical efficacy than small animal models.[151] Indeed, use of large animal models is recommended and sometimes required by the FDA, the European Medicines Agency (EMA), and the International Society for Stem Cell Research (ISSCR) to expedite testing and final commercial approval, especially for biological drugs.[151] RGI is of particular value for large animal imaging: (1) fewer animals are needed for experiments because the transgene, and therefore the vector bearing the transgene, can be tracked noninvasively, negating the need for multiple time points for tissue collection; and (2) each animal can serve as its own control by imaging prior to vector administration, thus reducing the number of animals needed and eliminating inter-animal variability. Cost is a significant limitation for large animal studies, so reducing the number of animals required will make large animal imaging more accessible. OI techniques used for small animals cannot be applied to large animals because visible light cannot penetrate the tissue mass of large animals.[27–29] Therefore, deep-tissue imaging modalities like SPECT, PET, and MRI must be used. To date, the only reporter gene to be repeatedly used for large animal deep-tissue imaging of OV or gene therapy is NIS, which has been studied in dogs, pigs, and non-human primates.[30,61,70–76] Use of the other genes discussed in this review for large animal imaging of OV and gene therapy is skewed heavily toward gene therapy and is sporadic.[87,152–161] The one exception is GFP, which has been used widely to test ocular gene therapies in dogs, cats, and non-human primates, because OI is possible due to the unique location and physiology of the eye.[162–168] Most recent research using HSV1-tk is directed toward cell therapies.[169–173] The use of deep-tissue imaging modalities for large animals is also much more translatable to human trials than OI, increasing the value of large animal imaging for pre-clinical validation. Further development of RGI methods for large animals will facilitate efficient translation of novel therapeutics.

THE FUTURE OF RGI

Oncolytic virotherapy and gene therapy are poised to revolutionize modern medicine in the coming decades. RGI offers a powerful modality for tracking oncolytic viruses and gene therapies but is vastly underutilized. This has been partially due to cost and access issues but may also stem from a lack of appreciation as to what can be achieved with RGI, particularly with regard to the rapid assessment of vector or virus biodistribution and durability of transgene expression in living animals. Detection sensitivity for many RGI systems has increased to the point that transgene expression can now be readily detected below the threshold that is necessary for clinical relevance, so while increasing sensitivity may improve imaging, this may not

translate to increased therapeutic benefit. Further sensitivity gains will doubtless be developed for most available RGI systems, but these enhancements may not be necessary to answer critical questions pertaining to the levels of gene expression needed for therapeutic benefit. Regardless, RGI itself has vastly improved since its inception at the turn of the century and continues to evolve and progress. As long as disease threatens human life, there will be a need to light up the therapies to eradicate it.

ACKNOWLEDGMENTS

We are grateful to the funding support from the National Institutes of Health (R44TR001191 and P50CA186781), the David F. and Margaret T. Grohne Family Foundation, and the Mayo Foundation.

AUTHOR CONTRIBUTIONS

S.C.C. and S.J.R. planned the manuscript. S.C.C. wrote the manuscript and created the figures. S.C.C., S.J.R., and K.W.P. reviewed and edited the manuscript. All authors reviewed and approved the final draft.

DECLARATION OF INTERESTS

S.J.R., K.W.P, and Mayo Clinic have a financial interest (equity) in the technologies described in this manuscript. S.J.R. and K.W.P. are cofounders of and hold equity in Imanis Life Sciences, LLC, a reporter gene imaging company. S.C.C. declares no competing interests.

REFERENCES

1. Russell, S.J., Peng, K.W., and Bell, J.C. (2012). Oncolytic virotherapy. Nat. Biotechnol. *30*, 658–670.
2. Russell, L., and Peng, K.W. (2018). The emerging role of oncolytic virus therapy against cancer. Linchuang Zhongliuxue Zazhi *7*, 16.
3. Alnasser, S.M. (2021). Review on mechanistic strategy of gene therapy in the treatment of disease. Gene *769*, 145246.
4. Cring, M.R., and Sheffield, V.C. (2020). Gene therapy and gene correction: targets, progress, and challenges for treating human diseases. Gene Ther. , Published online October 9, 2020. https://doi.org/10.1038/s41434-020-00197-8.
5. Leahy, M., Thompson, K., Zafar, H., Alexandrov, S., Foley, M., O'Flatharta, C., and Dockery, P. (2016). Functional imaging for regenerative medicine. Stem Cell Res. Ther. *7*, 57.
6. Willadsen, M., Chaise, M., Yarovoy, I., Zhang, A.Q., and Parashurama, N. (2018). Engineering molecular imaging strategies for regenerative medicine. Bioeng. Transl. Med. *3*, 232–255.
7. Martinez, O., Sosabowski, J., Maher, J., and Papa, S. (2019). New Developments in Imaging Cell-Based Therapy. J. Nucl. Med. *60*, 730–735.
8. Jung, S., and Chen, X. (2018). Quantum Dot-Dye Conjugates for Biosensing, Imaging, and Therapy. Adv. Healthc. Mater. *7*, e1800252.
9. Sheng, Y., Liao, L.D., Thakor, N.V., and Tan, M.C. (2014). Nanoparticles for molecular imaging. J. Biomed. Nanotechnol. *10*, 2641–2676.
10. Zelmer, A., and Ward, T.H. (2013). Noninvasive fluorescence imaging of small animals. J. Microsc. *252*, 8–15.
11. Sarder, P., Maji, D., and Achilefu, S. (2015). Molecular probes for fluorescence lifetime imaging. Bioconjug. Chem. *26*, 963–974.
12. Zhao, J., Jin, G., Weng, G., Li, J., Zhu, J., and Zhao, J. (2017). Recent advances in activatable fluorescence imaging probes for tumor imaging. Drug Discov. Today *22*, 1367–1374.
13. Xiao, Y.D., Paudel, R., Liu, J., Ma, C., Zhang, Z.S., and Zhou, S.K. (2016). MRI contrast agents: Classification and application (Review). Int. J. Mol. Med. *38*, 1319–1326.
14. Skinbjerg, M., Sibley, D.R., Javitch, J.A., and Abi-Dargham, A. (2012). Imaging the high-affinity state of the dopamine D2 receptor in vivo: fact or fiction? Biochem. Pharmacol. *83*, 193–198.
15. Morse, B., Al-Toubah, T., and Montilla-Soler, J. (2020). Anatomic and Functional Imaging of Neuroendocrine Tumors. Curr. Treat. Options Oncol. *21*, 75.
16. Derks, Y.H.W., Löwik, D.W.P.M., Sedelaar, J.P.M., Gotthardt, M., Boerman, O.C., Rijpkema, M., Lütje, S., and Heskamp, S. (2019). PSMA-targeting agents for radio- and fluorescence-guided prostate cancer surgery. Theranostics *9*, 6824–6839.
17. Pereira, S.M., Herrmann, A., Moss, D., Poptani, H., Williams, S.R., Murray, P., and Taylor, A. (2016). Evaluating the effectiveness of transferrin receptor-1 (TfR1) as a magnetic resonance reporter gene. Contrast Media Mol. Imaging *11*, 236–244.
18. Arena, F., Singh, J.B., Gianolio, E., Stefanìa, R., and Aime, S. (2011). β-Gal gene expression MRI reporter in melanoma tumor cells. Design, synthesis, and in vitro and in vivo testing of a Gd(III) containing probe forming a high relaxivity, melanin-like structure upon β-Gal enzymatic activation. Bioconjug. Chem. *22*, 2625–2635.
19. Likar, Y., Zurita, J., Dobrenkov, K., Shenker, L., Cai, S., Neschadim, A., Medin, J.A., Sadelain, M., Hricak, H., and Ponomarev, V. (2010). A new pyrimidine-specific reporter gene: a mutated human deoxycytidine kinase suitable for PET during treatment with acycloguanosine-based cytotoxic drugs. J. Nucl. Med. *51*, 1395–1403.
20. Lee, J.T., Zhang, H., Moroz, M.A., Likar, Y., Shenker, L., Sumzin, N., Lobo, J., Zurita, J., Collins, J., van Dam, R.M., and Ponomarev, V. (2017). Comparative Analysis of Human Nucleoside Kinase-Based Reporter Systems for PET Imaging. Mol. Imaging Biol. *19*, 100–108.
21. Campbell, D.O., Yaghoubi, S.S., Su, Y., Lee, J.T., Auerbach, M.S., Herschman, H., Satyamurthy, N., Czernin, J., Lavie, A., and Radu, C.G. (2012). Structure-guided engineering of human thymidine kinase 2 as a positron emission tomography reporter gene for enhanced phosphorylation of non-natural thymidine analog reporter probe. J. Biol. Chem. *287*, 446–454.
22. Patrick, P.S., Hammersley, J., Loizou, L., Kettunen, M.I., Rodrigues, T.B., Hu, D.E., Tee, S.S., Hesketh, R., Lyons, S.K., Soloviev, D., et al. (2014). Dual-modality gene reporter for in vivo imaging. Proc. Natl. Acad. Sci. USA *111*, 415–420.
23. Patrick, P.S., Rodrigues, T.B., Kettunen, M.I., Lyons, S.K., Neves, A.A., and Brindle, K.M. (2016). Development of Timd2 as a reporter gene for MRI. Magn. Reson. Med. *75*, 1697–1707.
24. Beinat, C., Alam, I.S., James, M.L., Srinivasan, A., and Gambhir, S.S. (2017). Development of [^{18}F]DASA-23 for Imaging Tumor Glycolysis Through Noninvasive Measurement of Pyruvate Kinase M2. Mol. Imaging Biol. *19*, 665–672.
25. Wu, M.R., Liu, H.M., Lu, C.W., Shen, W.H., Lin, I.J., Liao, L.W., Huang, Y.Y., Shieh, M.J., and Hsiao, J.K. (2018). Organic anion-transporting polypeptide 1B3 as a dual reporter gene for fluorescence and magnetic resonance imaging. FASEB J. *32*, 1705–1715.
26. Lau, J., Rousseau, J., Kwon, D., Bénard, F., and Lin, K.S. (2020). A Systematic Review of Molecular Imaging Agents Targeting Bradykinin B1 and B2 Receptors. Pharmaceuticals (Basel) *13*, 199.
27. Wu, Z.J., Tang, F.R., Ma, Z.W., Peng, X.C., Xiang, Y., Zhang, Y., Kang, J., Ji, J., Liu, X.Q., Wang, X.W., et al. (2018). Oncolytic Viruses for Tumor Precision Imaging and Radiotherapy. Hum. Gene Ther. *29*, 204–222.
28. Li, M., Wang, Y., Liu, M., and Lan, X. (2018). Multimodality reporter gene imaging: Construction strategies and application. Theranostics *8*, 2954–2973.
29. Serganova, I., and Blasberg, R.G. (2019). Molecular Imaging with Reporter Genes: Has Its Promise Been Delivered? J. Nucl. Med. *60*, 1665–1681.
30. Moulay, G., Ohtani, T., Ogut, O., Guenzel, A., Behfar, A., Zakeri, R., Haines, P., Storlie, J., Bowen, L., Pham, L., et al. (2015). Cardiac AAV9 Gene Delivery Strategies in Adult Canines: Assessment by Long-term Serial SPECT Imaging of Sodium Iodide Symporter Expression. Mol. Ther. *23*, 1211–1221.
31. Yamamoto, M., and Curiel, D.T. (2010). Current issues and future directions of oncolytic adenoviruses. Mol. Ther. *18*, 243–250.

32. Pelin, A., Wang, J., Bell, J., and Le Boeuf, F. (2018). The importance of imaging strategies for pre-clinical and clinical in vivo distribution of oncolytic viruses. Oncolytic Virother. *7*, 25–35.

33. Cotrim, A.P., and Baum, B.J. (2008). Gene therapy: some history, applications, problems, and prospects. Toxicol. Pathol. *36*, 97–103.

34. Weber, G.F. (2013). Gene therapy–why can it fail? Med. Hypotheses *80*, 613–616.

35. Wirth, T., Parker, N., and Ylä-Herttuala, S. (2013). History of gene therapy. Gene *525*, 162–169.

36. Histed, S.N., Lindenberg, M.L., Mena, E., Turkbey, B., Choyke, P.L., and Kurdziel, K.A. (2012). Review of functional/anatomical imaging in oncology. Nucl. Med. Commun. *33*, 349–361.

37. Bybel, B., Brunken, R.C., DiFilippo, F.P., Neumann, D.R., Wu, G., and Cerqueira, M.D. (2008). SPECT/CT imaging: clinical utility of an emerging technology. Radiographics *28*, 1097–1113.

38. Cherry, S.R., Sorenson, J.A., and Phelps, M.E. (2012). Physics in Nuclear Medicine, Fourth Edition (Elsevier Saunders), p. 279.

39. Phelps, M.E. (2000). Positron emission tomography provides molecular imaging of biological processes. Proc. Natl. Acad. Sci. USA *97*, 9226–9233.

40. Mettler, F.A., Jr., and Guiberteau, M.J. (2018). Essentials of Nuclear Medicine and Molecular Imaging, Seventh Edition (Elsevier Saunders), pp. 1–18.

41. McRobbie, D.W., Moore, A., Graves, M.J., and Prince, M.R. (2007). MRI from picture to proton (Cambridge University Press), pp. 137–161.

42. Concilio, S.C., Suksanpaisan, L., Pham, L., Peng, K.W., and Russell, S.J. (2021). Improved Noninvasive In Vivo Tracking of AAV-9 Gene Therapy Using the Perchlorate-Resistant Sodium Iodide Symporter from Minke Whale. Mol. Ther. *29*, 236–243.

43. Liu, X., Huang, H., Gao, Y., Zhou, L., Yang, J., Li, X., Li, Y., Zhao, H., Su, S., Ke, C., and Pei, Z. (2020). Visualization of gene therapy with a liver cancer-targeted adeno-associated virus 3 vector. J. Cancer *11*, 2192–2200.

44. Jia, Z.Y., Deng, H.F., Huang, R., Yang, Y.Y., Yang, X.C., Qi, Z.Z., and Ou, X.H. (2011). In vitro and in vivo studies of adenovirus-mediated human norepinephrine transporter gene transduction to hepatocellular carcinoma. Cancer Gene Ther. *18*, 196–205.

45. Wang, J., Arulanandam, R., Wassenaar, R., Falls, T., Petryk, J., Paget, J., Garson, K., Cemeus, C., Vanderhyden, B.C., Wells, R.G., et al. (2017). Enhancing Expression of Functional Human Sodium Iodide Symporter and Somatostatin Receptor in Recombinant Oncolytic Vaccinia Virus for In Vivo Imaging of Tumors. J. Nucl. Med. *58*, 221–227.

46. Wolff, J., and Maurey, J.R. (1963). Thyroidal iodide transport. IV. The role of ion size. Biochim. Biophys. Acta *69*, 58–67.

47. Van Sande, J., Massart, C., Beauwens, R., Schoutens, A., Costagliola, S., Dumont, J.E., and Wolff, J. (2003). Anion selectivity by the sodium iodide symporter. Endocrinology *144*, 247–252.

48. Cho, J.Y., Xing, S., Liu, X., Buckwalter, T.L., Hwa, L., Sferra, T.J., Chiu, I.M., and Jhiang, S.M. (2000). Expression and activity of human Na+/I- symporter in human glioma cells by adenovirus-mediated gene delivery. Gene Ther. *7*, 740–749.

49. Dingli, D., Peng, K.W., Harvey, M.E., Greipp, P.R., O'Connor, M.K., Cattaneo, R., Morris, J.C., and Russell, S.J. (2004). Image-guided radiovirotherapy for multiple myeloma using a recombinant measles virus expressing the thyroidal sodium iodide symporter. Blood *103*, 1641–1646.

50. Msaouel, P., Opyrchal, M., Dispenzieri, A., Peng, K.W., Federspiel, M.J., Russell, S.J., and Galanis, E. (2018). Clinical Trials with Oncolytic Measles Virus: Current Status and Future Prospects. Curr. Cancer Drug Targets *18*, 177–187.

51. Haddad, D., Chen, C.H., Carlin, S., Silberhumer, G., Chen, N.G., Zhang, Q., Longo, V., Carpenter, S.G., Mittra, A., Carson, J., et al. (2012). Imaging characteristics, tissue distribution, and spread of a novel oncolytic vaccinia virus carrying the human sodium iodide symporter. PLoS ONE *7*, e41647.

52. Goel, A., Carlson, S.K., Classic, K.L., Greiner, S., Naik, S., Power, A.T., Bell, J.C., and Russell, S.J. (2007). Radioiodide imaging and radiovirotherapy of multiple myeloma using VSV(Δ51)-NIS, an attenuated vesicular stomatitis virus encoding the sodium iodide symporter gene. Blood *110*, 2342–2350.

53. Bishnoi, S., Tiwari, R., Gupta, S., Byrareddy, S.N., and Nayak, D. (2018). Oncotargeting by Vesicular Stomatitis Virus (VSV): Advances in Cancer Therapy. Viruses *10*, 90.

54. Li, H., Nakashima, H., Decklever, T.D., Nace, R.A., and Russell, S.J. (2013). HSV-NIS, an oncolytic herpes simplex virus type 1 encoding human sodium iodide symporter for preclinical prostate cancer radiovirotherapy. Cancer Gene Ther. *20*, 478–485.

55. Miller, A., and Russell, S.J. (2016). The use of the NIS reporter gene for optimizing oncolytic virotherapy. Expert Opin. Biol. Ther. *16*, 15–32.

56. Barton, K.N., Xia, X., Yan, H., Stricker, H., Heisey, G., Yin, F.F., Nagaraja, T.N., Zhu, G., Kolozsvary, A., Fenstermacher, J.D., et al. (2004). A quantitative method for measuring gene expression magnitude and volume delivered by gene therapy vectors. Mol. Ther. *9*, 625–631.

57. Yang, H.S., Lee, H., Kim, S.J., Lee, W.W., Yang, Y.J., Moon, D.H., and Park, S.W. (2004). Imaging of human sodium-iodide symporter gene expression mediated by recombinant adenovirus in skeletal muscle of living rats. Eur. J. Nucl. Med. Mol. Imaging *31*, 1304–1311.

58. Boutagy, N.E., Ravera, S., Papademetris, X., Onofrey, J.A., Zhuang, Z.W., Wu, J., Feher, A., Stacy, M.R., French, B.A., Annex, B.H., et al. (2019). Noninvasive In Vivo Quantification of Adeno-Associated Virus Serotype 9-Mediated Expression of the Sodium/Iodide Symporter Under Hindlimb Ischemia and Neuraminidase Desialylation in Skeletal Muscle Using Single-Photon Emission Computed Tomography/Computed Tomography. Circ. Cardiovasc. Imaging *12*, e009063.

59. Miyagawa, M., Beyer, M., Wagner, B., Anton, M., Spitzweg, C., Gansbacher, B., Schwaiger, M., and Bengel, F.M. (2005). Cardiac reporter gene imaging using the human sodium/iodide symporter gene. Cardiovasc. Res. *65*, 195–202.

60. Miyagawa, M., Anton, M., Wagner, B., Haubner, R., Souvatzoglou, M., Gansbacher, B., Schwaiger, M., and Bengel, F.M. (2005). Non-invasive imaging of cardiac transgene expression with PET: comparison of the human sodium/iodide symporter gene and HSV1-tk as the reporter gene. Eur. J. Nucl. Med. Mol. Imaging *32*, 1108–1114.

61. Hickey, R.D., Mao, S.A., Glorioso, J., Elgilani, F., Amiot, B., Chen, H., Rinaldo, P., Marler, R., Jiang, H., DeGrado, T.R., et al. (2016). Curative ex vivo liver-directed gene therapy in a pig model of hereditary tyrosinemia type 1. Sci. Transl. Med. *8*, 349ra99.

62. Niu, G., Krager, K.J., Graham, M.M., Hichwa, R.D., and Domann, F.E. (2005). Noninvasive radiological imaging of pulmonary gene transfer and expression using the human sodium iodide symporter. Eur. J. Nucl. Med. Mol. Imaging *32*, 534–540.

63. Jiang, H., Bansal, A., Pandey, M.K., Peng, K.W., Suksanpaisan, L., Russell, S.J., and DeGrado, T.R. (2016). Synthesis of 18F-Tetrafluoroborate via Radiofluorination of Boron Trifluoride and Evaluation in a Murine C6-Glioma Tumor Model. J. Nucl. Med. *57*, 1454–1459.

64. Jiang, H., Bansal, A., Goyal, R., Peng, K.W., Russell, S.J., and DeGrado, T.R. (2018). Synthesis and evaluation of ^{18}F-hexafluorophosphate as a novel PET probe for imaging of sodium/iodide symporter in a murine C6-glioma tumor model. Bioorg. Med. Chem. *26*, 225–231.

65. Jiang, H., and DeGrado, T.R. (2018). [^{18}F]Tetrafluoroborate ([^{18}F]TFB) and its analogs for PET imaging of the sodium/iodide symporter. Theranostics *8*, 3918–3931.

66. Jiang, H., Schmit, N.R., Koenen, A.R., Bansal, A., Pandey, M.K., Glynn, R.B., Kemp, B.J., Delaney, K.L., Dispenzieri, A., Bakkum-Gamez, J.N., et al. (2017). Safety, pharmacokinetics, metabolism and radiation dosimetry of ^{18}F-tetrafluoroborate (^{18}F-TFB) in healthy human subjects. EJNMMI Res. *7*, 90.

67. Josefsson, M., Grunditz, T., Ohlsson, T., and Ekblad, E. (2002). Sodium/iodide-symporter: distribution in different mammals and role in entero-thyroid circulation of iodide. Acta Physiol. Scand. *175*, 129–137.

68. Concilio, S.C., Zhekova, H.R., Noskov, S.Y., and Russell, S.J. (2020). Inter-species variation in monovalent anion substrate selectivity and inhibitor sensitivity in the sodium iodide symporter (NIS). PLoS ONE *15*, e0229085.

69. Portulano, C., Paroder-Belenitsky, M., and Carrasco, N. (2014). The Na+/I- symporter (NIS): mechanism and medical impact. Endocr. Rev. *35*, 106–149.

70. Dwyer, R.M., Schatz, S.M., Bergert, E.R., Myers, R.M., Harvey, M.E., Classic, K.L., Blanco, M.C., Frisk, C.S., Marler, R.J., Davis, B.J., et al. (2005). A preclinical large animal model of adenovirus-mediated expression of the sodium-iodide symporter

for radioiodide imaging and therapy of locally recurrent prostate cancer. Mol. Ther. *12*, 835–841.

71. Lee, A.R., Woo, S.K., Kang, S.K., Lee, S.Y., Lee, M.Y., Park, N.W., Song, S.H., Lee, S.Y., Nahm, S.S., Yu, J.E., et al. (2015). Adenovirus-mediated expression of human sodium-iodide symporter gene permits in vivo tracking of adipose tissue-derived stem cells in a canine myocardial infarction model. Nucl. Med. Biol. *42*, 621–629.

72. Naik, S., Galyon, G.D., Jenks, N.J., Steele, M.B., Miller, A.C., Allstadt, S.D., Suksanpaisan, L., Peng, K.W., Federspiel, M.J., Russell, S.J., and LeBlanc, A.K. (2018). Comparative Oncology Evaluation of Intravenous Recombinant Oncolytic Vesicular Stomatitis Virus Therapy in Spontaneous Canine Cancer. Mol. Cancer Ther. *17*, 316–326.

73. Punzón, I., Mauduit, D., Holvoet, B., Thibaud, J.L., de Fornel, P., Deroose, C.M., Blanchard-Gutton, N., Vilquin, J.T., Sampaolesi, M., Barthélémy, I., and Blot, S. (2020). *In Vivo* Myoblasts Tracking Using the Sodium Iodide Symporter Gene Expression in Dogs. Mol. Ther. Methods Clin. Dev. *17*, 317–327.

74. Templin, C., Zweigerdt, R., Schwanke, K., Olmer, R., Ghadri, J.R., Emmert, M.Y., Müller, E., Küest, S.M., Cohrs, S., Schibli, R., et al. (2012). Transplantation and tracking of human-induced pluripotent stem cells in a pig model of myocardial infarction: assessment of cell survival, engraftment, and distribution by hybrid single photon emission computed tomography/computed tomography of sodium iodide symporter transgene expression. Circulation *126*, 430–439.

75. Velazquez-Salinas, L., Naik, S., Pauszek, S.J., Peng, K.W., Russell, S.J., and Rodriguez, L.L. (2017). Oncolytic Recombinant Vesicular Stomatitis Virus (VSV) Is Nonpathogenic and Nontransmissible in Pigs, a Natural Host of VSV. Hum. Gene Ther. Clin. Dev. *28*, 108–115.

76. Ostrominski, J.W., Yada, R.C., Sato, N., Klein, M., Blinova, K., Patel, D., Valadez, R., Palisoc, M., Pittaluga, S., Peng, K.W., et al. (2020). CRISPR/Cas9-mediated introduction of the sodium/iodide symporter gene enables noninvasive in vivo tracking of induced pluripotent stem cell-derived cardiomyocytes. Stem Cells Transl. Med. *9*, 1203–1217.

77. Mitrofanova, E., Unfer, R., Vahanian, N., and Link, C. (2006). Rat sodium iodide symporter allows using lower dose of 131I for cancer therapy. Gene Ther. *13*, 1052–1056.

78. Hu, S., Cao, W., Lan, X., He, Y., Lang, J., Li, C., Hu, J., An, R., Gao, Z., and Zhang, Y. (2011). Comparison of rNIS and hNIS as reporter genes for noninvasive imaging of bone mesenchymal stem cells transplanted into infarcted rat myocardium. Mol. Imaging *10*, 227–237.

79. Suksanpaisan, L., Pham, L., McIvor, S., Russell, S.J., and Peng, K.W. (2013). Oral contrast enhances the resolution of in-life NIS reporter gene imaging. Cancer Gene Ther. *20*, 638–641.

80. Kim, Y.H., Youn, H., Na, J., Hong, K.J., Kang, K.W., Lee, D.S., and Chung, J.K. (2015). Codon-optimized human sodium iodide symporter (opt-hNIS) as a sensitive reporter and efficient therapeutic gene. Theranostics *5*, 86–96.

81. Gambhir, S.S., Barrio, J.R., Wu, L., Iyer, M., Namavari, M., Satyamurthy, N., Bauer, E., Parrish, C., MacLaren, D.C., Borghei, A.R., et al. (1998). Imaging of adenoviral-directed herpes simplex virus type 1 thymidine kinase reporter gene expression in mice with radiolabeled ganciclovir. J. Nucl. Med. *39*, 2003–2011.

82. Gambhir, S.S., Bauer, E., Black, M.E., Liang, Q., Kokoris, M.S., Barrio, J.R., Iyer, M., Namavari, M., Phelps, M.E., and Herschman, H.R. (2000). A mutant herpes simplex virus type 1 thymidine kinase reporter gene shows improved sensitivity for imaging reporter gene expression with positron emission tomography. Proc. Natl. Acad. Sci. USA *97*, 2785–2790.

83. Jacobs, A., Voges, J., Reszka, R., Lercher, M., Gossmann, A., Kracht, L., Kaestle, C., Wagner, R., Wienhard, K., and Heiss, W.D. (2001). Positron-emission tomography of vector-mediated gene expression in gene therapy for gliomas. Lancet *358*, 727–729.

84. Peñuelas, I., Mazzolini, G., Boán, J.F., Sangro, B., Martí-Climent, J., Ruiz, M., Ruiz, J., Satyamurthy, N., Qian, C., Barrio, J.R., et al. (2005). Positron emission tomography imaging of adenoviral-mediated transgene expression in liver cancer patients. Gastroenterology *128*, 1787–1795.

85. Dempsey, M.F., Wyper, D., Owens, J., Pimlott, S., Papanastassiou, V., Patterson, J., Hadley, D.M., Nicol, A., Rampling, R., and Brown, S.M. (2006). Assessment of 123I-FIAU imaging of herpes simplex viral gene expression in the treatment of glioma. Nucl. Med. Commun. *27*, 611–617.

86. Sangro, B., Mazzolini, G., Ruiz, M., Ruiz, J., Quiroga, J., Herrero, I., Qian, C., Benito, A., Larrache, J., Olagüe, C., et al. (2010). A phase I clinical trial of thymidine kinase-based gene therapy in advanced hepatocellular carcinoma. Cancer Gene Ther. *17*, 837–843.

87. Pañeda, A., Collantes, M., Beattie, S.G., Otano, I., Snapper, J., Timmermans, E., Guembe, L., Petry, H., Lanciego, J.L., Benito, A., et al. (2011). Adeno-associated virus liver transduction efficiency measured by in vivo [18F]FHBG positron emission tomography imaging in rodents and nonhuman primates. Hum. Gene Ther. *22*, 999–1009.

88. MacLaren, D.C., Toyokuni, T., Cherry, S.R., Barrio, J.R., Phelps, M.E., Herschman, H.R., and Gambhir, S.S. (2000). PET imaging of transgene expression. Biol. Psychiatry *48*, 337–348.

89. Haddad, D., and Fong, Y. (2015). Molecular imaging of oncolytic viral therapy. Mol. Ther. Oncolytics *1*, 14007.

90. Chen, N., Zhang, Q., Yu, Y.A., Stritzker, J., Brader, P., Schirbel, A., Samnick, S., Serganova, I., Blasberg, R., Fong, Y., and Szalay, A.A. (2009). A novel recombinant vaccinia virus expressing the human norepinephrine transporter retains oncolytic potential and facilitates deep-tissue imaging. Mol. Med. *15*, 144–151.

91. Sorensen, A., Mairs, R.J., Braidwood, L., Joyce, C., Conner, J., Pimlott, S., Brown, M., and Boyd, M. (2012). In vivo evaluation of a cancer therapy strategy combining HSV1716-mediated oncolysis with gene transfer and targeted radiotherapy. J. Nucl. Med. *53*, 647–654.

92. Zhang, Y., and Wang, J. (2020). Targeting uptake transporters for cancer imaging and treatment. Acta Pharm. Sin. B *10*, 79–90.

93. Pauwels, E., Van Aerde, M., Bormans, G., and Deroose, C.M. (2020). Molecular imaging of norepinephrine transporter-expressing tumors: current status and future prospects. Q. J. Nucl. Med. Mol. Imaging *64*, 234–249.

94. Ivanidze, J., Roytman, M., Sasson, A., Skafida, M., Fahey, T.J., 3rd, Osborne, J.R., and Dutruel, S.P. (2019). Molecular imaging and therapy of somatostatin receptor positive tumors. Clin. Imaging *56*, 146–154.

95. Xu, C., and Zhang, H. (2015). Somatostatin receptor based imaging and radionuclide therapy. BioMed Res. Int. *2015*, 917968.

96. Zinn, K.R., Buchsbaum, D.J., Chaudhuri, T.R., Mountz, J.M., Grizzle, W.E., and Rogers, B.E. (2000). Noninvasive monitoring of gene transfer using a reporter receptor imaged with a high-affinity peptide radiolabeled with 99mTc or 188Re. J. Nucl. Med. *41*, 887–895.

97. McCart, J.A., Mehta, N., Scollard, D., Reilly, R.M., Carrasquillo, J.A., Tang, N., Deng, H., Miller, M., Xu, H., Libutti, S.K., et al. (2004). Oncolytic vaccinia virus expressing the human somatostatin receptor SSTR2: molecular imaging after systemic delivery using 111In-pentetreotide. Mol. Ther. *10*, 553–561.

98. Singh, S.P., Han, L., Murali, R., Solis, L., Roth, J., Ji, L., Wistuba, I., and Kundra, V. (2011). SSTR2-based reporters for assessing gene transfer into non-small cell lung cancer: evaluation using an intrathoracic mouse model. Hum. Gene Ther. *22*, 55–64.

99. Lears, K.A., Parry, J.J., Andrews, R., Nguyen, K., Wadas, T.J., and Rogers, B.E. (2015). Adenoviral-mediated imaging of gene transfer using a somatostatin receptor-cytosine deaminase fusion protein. Cancer Gene Ther. *22*, 215–221.

100. Cotugno, G., Aurilio, M., Annunziata, P., Capalbo, A., Faella, A., Rinaldi, V., Strisciuglio, C., Di Tommaso, M., Aloj, L., and Auricchio, A. (2011). Noninvasive repetitive imaging of somatostatin receptor 2 gene transfer with positron emission tomography. Hum. Gene Ther. *22*, 189–196.

101. Serganova, I., Ponomarev, V., and Blasberg, R. (2007). Human reporter genes: potential use in clinical studies. Nucl. Med. Biol. *34*, 791–807.

102. Iordanova, B., Goins, W.F., Clawson, D.S., Hitchens, T.K., and Ahrens, E.T. (2013). Quantification of HSV-1-mediated expression of the ferritin MRI reporter in the mouse brain. Gene Ther. *20*, 589–596.

103. Qin, C., Cheng, K., Chen, K., Hu, X., Liu, Y., Lan, X., Zhang, Y., Liu, H., Xu, Y., Bu, L., et al. (2013). Tyrosinase as a multifunctional reporter gene for Photoacoustic/MRI/PET triple modality molecular imaging. Sci. Rep. *3*, 1490.

104. Meier, S., Gilad, A.A., Brandon, J.A., Qian, C., Gao, E., Abisambra, J.F., and Vandsburger, M. (2018). Non-invasive detection of adeno-associated viral gene

transfer using a genetically encoded CEST-MRI reporter gene in the murine heart. Sci. Rep. *8*, 4638.

105. Yang, C., Tian, R., Liu, T., and Liu, G. (2016). MRI Reporter Genes for Noninvasive Molecular Imaging. Molecules *21*, 580.

106. Genove, G., DeMarco, U., Xu, H., Goins, W.F., and Ahrens, E.T. (2005). A new transgene reporter for in vivo magnetic resonance imaging. Nat. Med. *11*, 450–454.

107. Ono, K., Fuma, K., Tabata, K., and Sawada, M. (2009). Ferritin reporter used for gene expression imaging by magnetic resonance. Biochem. Biophys. Res. Commun. *388*, 589–594.

108. Vande Velde, G., Rangarajan, J.R., Toelen, J., Dresselaers, T., Ibrahimi, A., Krylychkina, O., Vreys, R., Van der Linden, A., Maes, F., Debyser, Z., et al. (2011). Evaluation of the specificity and sensitivity of ferritin as an MRI reporter gene in the mouse brain using lentiviral and adeno-associated viral vectors. Gene Ther. *18*, 594–605.

109. Zheng, N., Su, P., Liu, Y., Wang, H., Nie, B., Fang, X., Xu, Y., Lin, K., Lv, P., He, X., et al. (2019). Detection of neural connections with ex vivo MRI using a ferritin-encoding trans-synaptic virus. Neuroimage *197*, 133–142.

110. James, M.L., and Gambhir, S.S. (2012). A molecular imaging primer: modalities, imaging agents, and applications. Physiol. Rev. *92*, 897–965.

111. Paproski, R.J., Forbrich, A.E., Wachowicz, K., Hitt, M.M., and Zemp, R.J. (2011). Tyrosinase as a dual reporter gene for both photoacoustic and magnetic resonance imaging. Biomed. Opt. Express *2*, 771–780.

112. Stritzker, J., Kirscher, L., Scadeng, M., Deliolanis, N.C., Morscher, S., Symvoulidis, P., Schaefer, K., Zhang, Q., Buckel, L., Hess, M., et al. (2013). Vaccinia virus-mediated melanin production allows MR and optoacoustic deep tissue imaging and laser-induced thermotherapy of cancer. Proc. Natl. Acad. Sci. USA *110*, 3316–3320.

113. Kirscher, L., Deán-Ben, X.L., Scadeng, M., Zaremba, A., Zhang, Q., Kober, C., Fehm, T.F., Razansky, D., Ntziachristos, V., Stritzker, J., and Szalay, A.A. (2015). Doxycycline Inducible Melanogenic Vaccinia Virus as Theranostic Anti-Cancer Agent. Theranostics *5*, 1045–1057.

114. Gilad, A.A., Winnard, P.T., Jr., van Zijl, P.C.M., and Bulte, J.W.M. (2007). Developing MR reporter genes: promises and pitfalls. NMR Biomed. *20*, 275–290.

115. Gilad, A.A., McMahon, M.T., Walczak, P., Winnard, P.T., Jr., Raman, V., van Laarhoven, H.W.M., Skoglund, C.M., Bulte, J.W.M., and van Zijl, P.C.M. (2007). Artificial reporter gene providing MRI contrast based on proton exchange. Nat. Biotechnol. *25*, 217–219.

116. Consolino, L., Anemone, A., Capozza, M., Carella, A., Irrera, P., Corrado, A., Dhakan, C., Bracesco, M., and Longo, D.L. (2020). Non-invasive Investigation of Tumor Metabolism and Acidosis by MRI-CEST Imaging. Front. Oncol. *10*, 161.

117. Farrar, C.T., Buhrman, J.S., Liu, G., Kleijn, A., Lamfers, M.L.M., McMahon, M.T., Gilad, A.A., and Fulci, G. (2015). Establishing the Lysine-rich Protein CEST Reporter Gene as a CEST MR Imaging Detector for Oncolytic Virotherapy. Radiology *275*, 746–754.

118. Taruttis, A., and Ntziachristos, V. (2012). Translational optical imaging. AJR Am. J. Roentgenol. *199*, 263–271.

119. Martelli, C., Lo Dico, A., Diceglie, C., Lucignani, G., and Ottobrini, L. (2016). Optical imaging probes in oncology. Oncotarget *7*, 48753–48787.

120. Pirovano, G., Roberts, S., Kossatz, S., and Reiner, T. (2020). Optical Imaging Modalities: Principles and Applications in Preclinical Research and Clinical Settings. J. Nucl. Med. *61*, 1419–1427.

121. Karda, R., Rahim, A.A., Wong, A.M.S., Suff, N., Diaz, J.A., Perocheau, D.P., Tijani, M., Ng, J., Baruteau, J., Martin, N.P., et al. (2020). Generation of light-producing somatic-transgenic mice using adeno-associated virus vectors. Sci. Rep. *10*, 2121.

122. Hutzen, B., Pierson, C.R., Russell, S.J., Galanis, E., Raffel, C., and Studebaker, A.W. (2012). Treatment of medulloblastoma using an oncolytic measles virus encoding the thyroidal sodium iodide symporter shows enhanced efficacy with radioiodine. BMC Cancer *12*, 508.

123. Filonov, G.S., Piatkevich, K.D., Ting, L.M., Zhang, J., Kim, K., and Verkhusha, V.V. (2011). Bright and stable near-infrared fluorescent protein for *in vivo* imaging. Nat. Biotechnol. *29*, 757–761.

124. Huang, C., Lan, W., Wang, F., Zhang, C., Liu, X., and Chen, Q. (2017). AAV-iRFP labelling of human mesenchymal stem cells for near-infrared fluorescence imaging. Biosci. Rep. *37*, BSR20160556.

125. Liu, Y., Zhang, H., Chen, R., Wu, Y., Yang, X., Liu, X., Zeng, S., and Guo, W. (2020). UnaG as a reporter in adeno-associated virus-mediated gene transfer for biomedical imaging. J. Biophotonics *13*, e202000182.

126. Love, A.C., and Prescher, J.A. (2020). Seeing (and Using) the Light: Recent Developments in Bioluminescence Technology. Cell Chem. Biol. *27*, 904–920.

127. Hall, M.P., Unch, J., Binkowski, B.F., Valley, M.P., Butler, B.L., Wood, M.G., Otto, P., Zimmerman, K., Vidugiris, G., Machleidt, T., et al. (2012). Engineered luciferase reporter from a deep sea shrimp utilizing a novel imidazopyrazinone substrate. ACS Chem. Biol. *7*, 1848–1857.

128. Sasaki, M., Anindita, P.D., Phongphaew, W., Carr, M., Kobayashi, S., Orba, Y., and Sawa, H. (2018). Development of a rapid and quantitative method for the analysis of viral entry and release using a NanoLuc luciferase complementation assay. Virus Res. *243*, 69–74.

129. Saito, K., Chang, Y.F., Horikawa, K., Hatsugai, N., Higuchi, Y., Hashida, M., Yoshida, Y., Matsuda, T., Arai, Y., and Nagai, T. (2012). Luminescent proteins for high-speed single-cell and whole-body imaging. Nat. Commun. *3*, 1262.

130. Suzuki, K., Kimura, T., Shinoda, H., Bai, G., Daniels, M.J., Arai, Y., Nakano, M., and Nagai, T. (2016). Five colour variants of bright luminescent protein for real-time multicolour bioimaging. Nat. Commun. *7*, 13718.

131. Chu, J., Oh, Y., Sens, A., Ataie, N., Dana, H., Macklin, J.J., Laviv, T., Welf, E.S., Dean, K.M., Zhang, F., et al. (2016). A bright cyan-excitable orange fluorescent protein facilitates dual-emission microscopy and enhances bioluminescence imaging in vivo. Nat. Biotechnol. *34*, 760–767.

132. Yeh, H.W., Karmach, O., Ji, A., Carter, D., Martins-Green, M.M., and Ai, H.W. (2017). Red-shifted luciferase-luciferin pairs for enhanced bioluminescence imaging. Nat. Methods *14*, 971–974.

133. Dixon, A.S., Schwinn, M.K., Hall, M.P., Zimmerman, K., Otto, P., Lubben, T.H., Butler, B.L., Binkowski, B.F., Machleidt, T., Kirkland, T.A., et al. (2016). NanoLuc Complementation Reporter Optimized for Accurate Measurement of Protein Interactions in Cells. ACS Chem. Biol. *11*, 400–408.

134. Mezzanotte, L., van 't Root, M., Karatas, H., Goun, E.A., and Löwik, C.W.G.M. (2017). In Vivo Molecular Bioluminescence Imaging: New Tools and Applications. Trends Biotechol. *35*, 640–652.

135. Gaspar, N., Zambito, G., Dautzenberg, I.J.C., Cramer, S.J., Hoeben, R.C., Lowik, C., Walker, J.R., Kirkland, T.A., Smith, T.P., van Weerden, W.M., et al. (2020). NanoBiT System and Hydrofurimazine for Optimized Detection of Viral Infection in Mice-A Novel in Vivo Imaging Platform. Int. J. Mol. Sci. *21*, 5863.

136. Nakayama, J., Saito, R., Hayashi, Y., Kitada, N., Tamaki, S., Han, Y., Semba, K., and Maki, S.A. (2020). High Sensitivity In Vivo Imaging of Cancer Metastasis Using a Near-Infrared Luciferin Analogue seMpai. Int. J. Mol. Sci. *21*, E7896.

137. de Jong, M., Essers, J., and van Weerden, W.M. (2014). Imaging preclinical tumour models: improving translational power. Nat. Rev. Cancer *14*, 481–493.

138. Guse, K., Dias, J.D., Bauerschmitz, G.J., Hakkarainen, T., Aavik, E., Ranki, T., Pisto, T., Särkioja, M., Desmond, R.A., Kanerva, A., and Hemminki, A. (2007). Luciferase imaging for evaluation of oncolytic adenovirus replication in vivo. Gene Ther. *14*, 902–911.

139. Rojas, J.J., Sampath, P., Hou, W., and Thorne, S.H. (2015). Defining Effective Combinations of Immune Checkpoint Blockade and Oncolytic Virotherapy. Clin. Cancer Res. *21*, 5543–5551.

140. Ciarrocchi, E., and Belcari, N. (2017). Cerenkov luminescence imaging: physics principles and potential applications in biomedical sciences. EJNMMI Phys. *4*, 14.

141. Robertson, R., Germanos, M.S., Li, C., Mitchell, G.S., Cherry, S.R., and Silva, M.D. (2009). Optical imaging of Cerenkov light generation from positron-emitting radiotracers. Phys. Med. Biol. *54*, N355–N365.

142. Ruggiero, A., Holland, J.P., Lewis, J.S., and Grimm, J. (2010). Cerenkov luminescence imaging of medical isotopes. J. Nucl. Med. *51*, 1123–1130.

143. Boschi, F., and Spinelli, A.E. (2020). Nanoparticles for Cerenkov and Radioluminescent Light Enhancement for Imaging and Radiotherapy. Nanomaterials (Basel) *10*, 1771.

144. Chin, P.T.K., Welling, M.M., Meskers, S.C.J., Valdes Olmos, R.A., Tanke, H., and van Leeuwen, F.W.B. (2013). Optical imaging as an expansion of nuclear medicine: Cerenkov-based luminescence vs fluorescence-based luminescence. Eur. J. Nucl. Med. Mol. Imaging *40*, 1283–1291.

145. Jacques, S.L. (2013). Optical properties of biological tissues: a review. Phys. Med. Biol. *58*, R37–R61.

146. Liu, H., Ren, G., Liu, S., Zhang, X., Chen, L., Han, P., and Cheng, Z. (2010). Optical imaging of reporter gene expression using a positron-emission-tomography probe. J. Biomed. Opt. *15*, 060505.

147. Zhang, H.F., Maslov, K., Stoica, G., and Wang, L.V. (2006). Functional photoacoustic microscopy for high-resolution and noninvasive in vivo imaging. Nat. Biotechnol. *24*, 848–851.

148. Tsang, V.T.C., Li, X., and Wong, T.T.W. (2020). A Review of Endogenous and Exogenous Contrast Agents Used in Photoacoustic Tomography with Different Sensing Configurations. Sensors (Basel) *20*, 5595.

149. Upputuri, P.K., and Pramanik, M. (2020). Recent advances in photoacoustic contrast agents for in vivo imaging. Wiley Interdiscip. Rev. Nanomed. Nanobiotechnol. *12*, e1618.

150. Huang, L.L., Li, X., Zhang, J., Zhao, Q.R., Zhang, M.J., Liu, A.A., Pang, D.W., and Xie, H.Y. (2019). MnCaCs-Biomineralized Oncolytic Virus for Bimodal Imaging-Guided and Synergistically Enhanced Anticancer Therapy. Nano Lett. *19*, 8002–8009.

151. Ribitsch, I., Baptista, P.M., Lange-Consiglio, A., Melotti, L., Patruno, M., Jenner, F., Schnabl-Feichter, E., Dutton, L.C., Connolly, D.J., van Steenbeek, F.G., et al. (2020). Large Animal Models in Regenerative Medicine and Tissue Engineering: To Do or Not to Do. Front. Bioeng. Biotechnol. *8*, 972.

152. Bankiewicz, K.S., Eberling, J.L., Kohutnicka, M., Jagust, W., Pivirotto, P., Bringas, J., Cunningham, J., Budinger, T.F., and Harvey-White, J. (2000). Convection-enhanced delivery of AAV vector in parkinsonian monkeys; in vivo detection of gene expression and restoration of dopaminergic function using pro-drug approach. Exp. Neurol. *164*, 2–14.

153. Bengel, F.M., Anton, M., Richter, T., Simoes, M.V., Haubner, R., Henke, J., Erhardt, W., Reder, S., Lehner, T., Brandau, W., et al. (2003). Noninvasive imaging of transgene expression by use of positron emission tomography in a pig model of myocardial gene transfer. Circulation *108*, 2127–2133.

154. Miyagawa, M., Anton, M., Haubner, R., Simoes, M.V., Städele, C., Erhardt, W., Reder, S., Lehner, T., Wagner, B., Noll, S., et al. (2004). PET of cardiac transgene expression: comparison of 2 approaches based on herpesviral thymidine kinase reporter gene. J. Nucl. Med. *45*, 1917–1923.

155. Tarantal, A.F., Lee, C.C.I., Jimenez, D.F., and Cherry, S.R. (2006). Fetal gene transfer using lentiviral vectors: in vivo detection of gene expression by microPET and optical imaging in fetal and infant monkeys. Hum. Gene Ther. *17*, 1254–1261.

156. Cunningham, J., Pivirotto, P., Bringas, J., Suzuki, B., Vijay, S., Sanftner, L., Kitamura, M., Chan, C., and Bankiewicz, K.S. (2008). Biodistribution of adeno-associated virus type-2 in nonhuman primates after convection-enhanced delivery to brain. Mol. Ther. *16*, 1267–1275.

157. Fontanellas, A., Hervas-Stubbs, S., Sampedro, A., Collantes, M., Azpilicueta, A., Mauleón, I., Pañeda, A., Quincoces, G., Prieto, J., Melero, I., and Peñuelas, I. (2009). PET imaging of thymidine kinase gene expression in the liver of non-human primates following systemic delivery of an adenoviral vector. Gene Ther. *16*, 136–141.

158. Tarantal, A.F., and Lee, C.C.I. (2010). Long-term luciferase expression monitored by bioluminescence imaging after adeno-associated virus-mediated fetal gene delivery in rhesus monkeys (Macaca mulatta). Hum. Gene Ther. *21*, 143–148.

159. Pouliot, F., Karanikolas, B.D.W., Johnson, M., Sato, M., Priceman, S.J., Stout, D., Sohn, J., Satyamurthy, N., deKernion, J.B., and Wu, L. (2011). In vivo imaging of intraprostatic-specific gene transcription by PET. J. Nucl. Med. *52*, 784–791.

160. Tarantal, A.F., Lee, C.C.I., Martinez, M.L., Asokan, A., and Samulski, R.J. (2017). Systemic and Persistent Muscle Gene Expression in Rhesus Monkeys with a Liver De-Targeted Adeno-Associated Virus Vector. Hum. Gene Ther. *28*, 385–391.

161. Watano, R., Ohmori, T., Hishikawa, S., Sakata, A., and Mizukami, H. (2020). Utility of microminipigs for evaluating liver-mediated gene expression in the presence of neutralizing antibody against vector capsid. Gene Ther. *27*, 427–434.

162. Borrás, T., Gabelt, B.T., Klintworth, G.K., Peterson, J.C., and Kaufman, P.L. (2001). Non-invasive observation of repeated adenoviral GFP gene delivery to the anterior segment of the monkey eye in vivo. J. Gene Med. *3*, 437–449.

163. Weber, M., Rabinowitz, J., Provost, N., Conrath, H., Folliot, S., Briot, D., Chérel, Y., Chenuaud, P., Samulski, J., Moullier, P., and Rolling, F. (2003). Recombinant adeno-associated virus serotype 4 mediates unique and exclusive long-term transduction of retinal pigmented epithelium in rat, dog, and nonhuman primate after subretinal delivery. Mol. Ther. *7*, 774–781.

164. Petersen-Jones, S.M., Bartoe, J.T., Fischer, A.J., Scott, M., Boye, S.L., Chiodo, V., and Hauswirth, W.W. (2009). AAV retinal transduction in a large animal model species: comparison of a self-complementary AAV2/5 with a single-stranded AAV2/5 vector. Mol. Vis. *15*, 1835–1842.

165. Yin, L., Greenberg, K., Hunter, J.J., Dalkara, D., Kolstad, K.D., Masella, B.D., Wolfe, R., Visel, M., Stone, D., Libby, R.T., et al. (2011). Intravitreal injection of AAV2 transduces macaque inner retina. Invest. Ophthalmol. Vis. Sci. *52*, 2775–2783.

166. Joussemet, B., Belbellaa, B., Mendes-Madeira, A., Bucher, T., Briot-Nivard, D., Dubreil, L., Colle, M.A., Cherel, Y., Moullier, P., and Rolling, F. (2011). Neonatal systemic delivery of scAAV9 in rodents and large animals results in gene transfer to RPE cells in the retina. Exp. Eye Res. *93*, 491–502.

167. Boye, S.E., Alexander, J.J., Witherspoon, C.D., Boye, S.L., Peterson, J.J., Clark, M.E., Sandefer, K.J., Girkin, C.A., Hauswirth, W.W., and Gamlin, P.D. (2016). Highly Efficient Delivery of Adeno-Associated Viral Vectors to the Primate Retina. Hum. Gene Ther. *27*, 580–597.

168. Boye, S.L., Choudhury, S., Crosson, S., Di Pasquale, G., Afione, S., Mellen, R., Makal, V., Calabro, K.R., Fajardo, D., Peterson, J., et al. (2020). Novel AAV44.9-Based Vectors Display Exceptional Characteristics for Retinal Gene Therapy. Mol. Ther. *28*, 1464–1478.

169. Greco, R., Oliveira, G., Stanghellini, M.T.L., Vago, L., Bondanza, A., Peccatori, J., Cieri, N., Marktel, S., Mastaglio, S., Bordignon, C., et al. (2015). Improving the safety of cell therapy with the TK-suicide gene. Front. Pharmacol. *6*, 95.

170. Barton, K.N., Stricker, H., Brown, S.L., Elshaikh, M., Aref, I., Lu, M., Pegg, J., Zhang, Y., Karvelis, K.C., Siddiqui, F., et al. (2008). Phase I study of noninvasive imaging of adenovirus-mediated gene expression in the human prostate. Mol. Ther. *16*, 1761–1769.

171. Russell, S.J., Federspiel, M.J., Peng, K.W., Tong, C., Dingli, D., Morice, W.G., Lowe, V., O'Connor, M.K., Kyle, R.A., Leung, N., et al. (2014). Remission of disseminated cancer after systemic oncolytic virotherapy. Mayo Clin. Proc. *89*, 926–933.

172. Eychenne, R., Bouvry, C., Bourgeois, M., Loyer, P., Benoist, E., and Lepareur, N. (2020). Overview of Radiolabeled Somatostatin Analogs for Cancer Imaging and Therapy. Molecules *25*, 4012.

173. Duwé, S., and Dedecker, P. (2019). Optimizing the fluorescent protein toolbox and its use. Curr. Opin. Biotechnol. *58*, 183–191.